



Technical note

Potential resistance to transgranular fatigue crack growth of Fe–C alloy with a supersaturated carbon clarified through FIB micro-notching technique



Bochuan Li^a, Motomichi Koyama^{a,*}, Eisaku Sakurada^b, Nobuyuki Yoshimura^c, Kohsaku Ushioda^c, Hiroshi Noguchi^a

^a Faculty of Engineering, Kyushu University, 744 Moto-oka, Nishi-ku, Fukuoka-shi, Fukuoka 819-0395, Japan

^b Nippon Steel & Sumitomo Metal Corporation, 5-3 Tokai, Tokai, Aichi 476-8686, Japan

^c Nippon Steel & Sumitomo Metal Corporation, 20-1 Shintomi, Futtsu, Chiba 293-8511, Japan

ARTICLE INFO

Article history:

Received 30 December 2015

Accepted 5 January 2016

Available online 11 January 2016

Keywords:

Threshold stress intensity factor range

Ferritic steel

Transgranular fatigue crack

Strain-age hardening

ABSTRACT

The threshold stress intensity factor range (ΔK_{th}) of water-quenched Fe–0.017C (wt.%) fully ferritic steel was determined using room-temperature fatigue tests on micro-notched specimens. The experimentally determined ΔK_{th} was approximately 40.5% higher than conventionally predicted results. This extraordinary resistance to transgranular fatigue crack propagation likely results from the strain-age hardening.

© 2016 Elsevier Ltd. All rights reserved.

1. Introduction

With the development of modern industry, the metal fatigue problem plays an increasingly important role in mechanical performance. To address this problem, some researchers [1,2] have focused on the mechanics viewpoint, where a more precise fatigue life can be predicted to increase the potential use of materials. Others [3–9] have contributed to enhancing the fatigue strength, especially the fatigue limit, using a metallurgy perspective. The fatigue limit associated with a non-propagating crack is attributed to microstructural characteristics [3,4], crack closure [5,6], and strain aging [7–9]. In particular, strain aging of carbon in steels, described as the interaction between dislocations and interstitial carbon, has been known to strengthen the vicinity of a non-propagating fatigue crack tip and prevent the crack from further propagation [9].

A significant amount of research has recently been devoted to better understanding of the effect of strain aging on the fatigue strength in steels [7–11]; however, most of these studies consider the degree of strain aging over a wide range of temperature and

attempt to find the definite strain-aging regime where the fatigue limit increases remarkably. In fact, there are at least four major factors affecting the strain-aging process under fatigue: the velocity of dislocation motion, waiting time for aging, solute atom diffusivity, and number of solute atoms [7]. The temperature clearly affects the diffusivity of solute atoms significantly. However, the effect of considerable solute atom content associated with strain-age hardening on fatigue strength has hardly been examined. Hence, to investigate the influence of solute carbon content on the fatigue strength, especially for the fatigue threshold of small fatigue cracks, we firstly focused on a water-quenched Fe–C (wt.%) binary alloy and an interstitial-free (IF) steel. More specifically, the former consists of a single ferritic phase where almost all carbon is in solution, and the latter is a ferritic steel nearly without solute carbon.

In our previous study, smooth specimens of the Fe–C binary alloy were studied [12]. The investigation clarified two facts: (1) transgranular crack propagation often stops in the grain interior even at high stress level and (2) the failure mechanism of the smooth specimen consists of intergranular crack initiation and propagation, most likely due to the lack of carbon segregation to the grain boundaries. However, the effect of strain-age hardening on the resistance to transgranular fatigue cracking cannot be quantitatively determined using the smooth specimens. These

* Corresponding author. Tel.: +81 92 802 3224.

E-mail address: koyama@mech.kyushu-u.ac.jp (M. Koyama).

facts indicate that the water-quenched Fe–C alloy has potential regarding resistance to transgranular fatigue crack propagation. Therefore, the aim of this paper is to quantify the influence of large interstitial carbon content on small-crack fatigue threshold ΔK_{th} corresponding to the resistance to transgranular fatigue cracking by introducing a micro-notch in a grain interior of the Fe–C binary alloy. Moreover, the obtained ΔK_{th} is compared with that of the IF steel by using the same micro-notch.

2. Experimental procedure

As mentioned above, a water quenched Fe–0.017C (wt.%) ferritic alloy and an interstitial-free steel were selected. As for Fe–C steel in the present study, the full chemical composition was C = 0.017, Si \leq 0.003, Mn \leq 0.003, P \leq 0.002, S \leq 0.0003, Ti \leq 0.002, Al = 0.052, and N = 0.0009 (wt.%), which had the simplest chemical composition and microstructure. First, the specimen was solution-treated for 1 h at 700 °C and then water quenched to keep carbon in supersaturated solid solution at room temperature and to suppress the formation of carbon cluster or carbides and uncontrolled carbon segregation. The heat-treated specimen had a grain size of approximately 65 μ m. The specimens were always stored in a refrigerator at –87 °C except during sample preparation and testing to inhibit precipitation and carbon segregation to the largest extent. By contrast, IF steel, in which the chemical composition was C = 0.0019, Si = 0.009, Mn \leq 0.003, P \leq 0.002, S \leq 0.0003, Ti = 0.029, Al = 0.028, N = 0.0008 and O = 0.0015 (wt.%), was produced to completely fix C and N as Ti(CN) so that there were no interstitial solute atoms.

Fatigue tests for these two materials were conducted using an Ono-type rotating bending fatigue testing machine with a stress ratio of –1 and frequency 50 Hz in air at room temperature. The specimen shape is shown in Fig. 1. Three types of artificial flaws were introduced in the specimen. Type A flaw was introduced using focused ion beam (FIB) milling, and types B and C flaws were introduced using a combination of drilling and FIB. The three flaws were applied for the Fe–0.017C alloy, while flaw A and flaw C were applied for the IF steel. The corresponding dimensions of these flaws are also described in Fig. 1. The fatigue crack growth was examined using the replica method with an optical microscope. The fatigue limit of the smooth specimen of the Fe–C alloy was 210 MPa, corresponding to 10^7 cycles, according to previous result [12].

3. Capability of Murakami's equation and definition of $\sqrt{\text{area}}$ for irregular flaw

In order to estimate the growth degree of the threshold stress intensity factor range ΔK_{th} of Fe–0.017C alloy and IF steel, Murakami's equation, which only requires the Vickers hardness HV and $\sqrt{\text{area}}$ of the flaw to predict the small notch or crack threshold, is used as the reference standard [13]:

$$\Delta K_{th} = 0.65 \times 2\sigma_w \sqrt{\pi \sqrt{\text{area}}} \quad (R = -1) \quad (1)$$

$$\Delta K_{th_pre} = 3.3 \times 10^{-3} (HV + 120) (\sqrt{\text{area}})^{1/3} \quad (R = -1) \quad (2)$$

$$I\% = \frac{\Delta K_{th} - \Delta K_{th_pre}}{\Delta K_{th_pre}} \times 100\% \quad (3)$$

where σ_w and $\sqrt{\text{area}}$ are the fatigue crack non-propagation limit and the square root of the area obtained by projecting the flaw onto a plane perpendicular to the loading axis direction, respectively. ΔK_{th_pre} is the predicted ΔK_{th} , and I is the predicted deviation of the experimental result from the predicted result.

In fact, Murakami's equation can not only be used to predict fatigue crack non-propagation limit from a non-metallic inclusion, but also be used to predict the small crack ΔK_{th} for various materials including carbon steels. The capability of its prediction accuracy is shown in Fig. 3(a). All the experimental data in various materials with different initial notch geometries fall within the 10% error interval band. Therefore, it is reasonable to regard this equation as a reference standard for a comparison with the present ferritic steels.

In addition, in terms of irregular shape flaw such as types B and C, the definition of $\sqrt{\text{area}}$ must be clear. Fig. 2(a) shows a result of the finite element analysis for the irregular shape flaw with the remote stress 100 MPa and the loading direction is perpendicular to the cross section. Fig. 2(b) is the corresponding schematic. It can be seen from Fig. 2(b) that points A and E have the maximum stress concentration. Namely, crack initiates from the maximum stress concentration points and be inclined to become smoothly contoured crack after propagation and subsequent non-propagation [14]. Hence, $\sqrt{\text{area}}$ for the irregular shape flaw in this paper is defined to be the contour DBCIGFHD in Fig. 2(b), which is similar with that in the previous study [15].

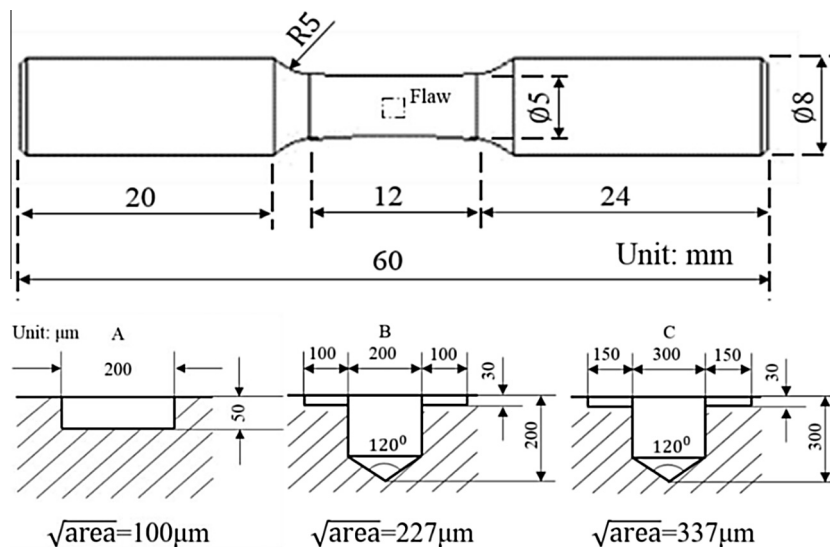


Fig. 1. Geometries of the specimen and artificial flaws.

Download English Version:

<https://daneshyari.com/en/article/778067>

Download Persian Version:

<https://daneshyari.com/article/778067>

[Daneshyari.com](https://daneshyari.com)